

## iPS cell transplantation in a mouse model – A semiquantitative assessment

Patrick Yit Han Ong <sup>a</sup>, Zanariah Hashim <sup>a</sup>, Mohd Effendy Abd Wahid <sup>b</sup>, Diana Bee Lan Ong <sup>c</sup>, Nur Adibah Bakkerly <sup>c</sup>, Reena Rahayu Md Zin <sup>d</sup>, Nur Maya Sabrina Tizen Liam <sup>d</sup>, Faridah Abd Rahman <sup>d</sup>, Muaatamarulain Mustangin <sup>d</sup>, Norazwin Hajri <sup>e</sup>, Fadzilah Adibah Abdul Majid <sup>e,\*</sup>

<sup>a</sup> Department of Bioprocess & Polymer Engineering, School of Chemical and Energy Engineering, Faculty of Engineering, Universiti Teknologi Malaysia, 81310, UTM Johor Bahru, Johor, Malaysia

<sup>b</sup> School of Fisheries and Aquaculture, Universiti Malaysia Terengganu, 21030, Kuala Terengganu, Terengganu, Malaysia

<sup>c</sup> Pathology's Unit for Research Support and Education, Department of Pathology, Faculty of Medicine, Universiti Malaysia, 50603, Kuala Lumpur, Wilayah Persekutuan Kuala Lumpur, Malaysia

<sup>d</sup> Department of Pathology, Faculty of Medicine, Universiti Kebangsaan Malaysia, 56000, Cheras, Wilayah Persekutuan Kuala Lumpur, Malaysia

<sup>e</sup> Institute of Marine Biotechnology, Universiti Malaysia Terengganu, 21030, Kuala Terengganu, Terengganu, Malaysia

\* Corresponding author: f.adibah@umt.edu.my

### Article history

Received 3 February 2020

Revised 17 March 2020

Accepted 9 September 2020

Published Online 24 December 2020

### Abstract

This study was carried out to determine the effectiveness of induced pluripotent stem (iPS) cell transplantation as a therapy on wound healing using a splinted wound mouse model. Eighteen clinically healthy female mice were treated with 1µg/g of dexamethasone intramuscular injection once a day for three consecutive days to induce immunosuppression. Under anaesthesia, two sterile wounds were made on shaved backs of each mouse via biopsy punch. With a gap of 20 mm in-between, six injections were delivered once, around the two wounds before the wounds were adhered with splints and wound dressing. The mice were divided into two groups; Group A was given  $7 \times 10^5$  iPS cells in each injection, and while Group B were injected with 0.9% sodium chloride instead. Wound closure rates were determined through timed scaled photography and analyses with GNU Image Manipulation Program. Three mice from each group were euthanised every 7 days post-wounding, immediately after which wound beds and blood were harvested. Wound beds were fixed, processed, blocked, and sectioned. Sections were stained with H&E; Masson's Trichrome; and immunolabeled for CD31 and CD68; and then examined under a compound microscope subjected to a scoring scheme. From this semiquantitative assessment, Group A sections scored better in angiogenesis on day 7 ( $p = 0.057$ ), a vital process in the proliferation stage, and hypodermis regeneration on day 21 ( $p = 0.006$ ), which suggests the wound healing is complete. Together, these findings suggest Group A was ahead in the process of wound healing; although results from lymphocyte count, fibroblast count, granulation tissue, collagen, and wound closure were not statistically significant.

**Keywords:** Wound and Injuries, Induced Pluripotent Stem Cells, Skin, Transplants, Cell Transplantation

© 2020 Penerbit UTM Press. All rights reserved

## INTRODUCTION

Stem cells, given their differential potency and ability to self-replicate, represents an interesting 'new' approach of treating wounds. At least five independent groups have investigated the use of either bone marrow-derived cells or mesenchymal stem cells in wound treatment and found the treatments effective to varying degrees [1–5]. In theory, bone marrow-derived cells or mesenchymal stem cells are limited by their cell potency and cannot contribute to the formation of all components of the skin; skin components are of either ectodermal or mesodermal lineage, yet bone marrow-derived cells and mesenchymal stem cells are branches of the mesoderm lineage, making them incapable of differentiating into cells of the ectoderm lineage. While it is true that mesenchymal stem cells have been differentiated into neuronal tissue (of ectodermal lineage), their functionality as neurons remain in question [6].

For the derivation of all skin components, pluripotent stem cells may be more suitable. In fact, embryonic stem (ES) cells have been applied and found to be effective in wounds treatment of diabetic rats

[7]. However, ES cells are often associated with ethical concerns as their derivation requires the destruction of a blastocyst-stage embryo.

Alternatively, iPS cells, a type of stem cells with differential potency equivalent to that of ES cells, should be considered and studied. Unlike ES cells, iPS cells can be generated by forced-expression of four transcription factors in somatic cells [8], therefore side-stepping ethical complications associated with ES cells. On top of that, the use of iPS cells could also address the issue of transplantation rejection as patient-homologous iPS cells can be generated from a patient's own cells. Yet, despite the many advantages iPS cells offer, research of their application on wound therapy has been lacking.

## MATERIALS AND METHODS

### APS0004 Cell Culture

APS0004, a line of iPS cells generated from embryonic fibroblasts of a male mouse, was maintained on mitotically-inactivated SNL 76/7 cell (CellBioLabs Inc, San Diego: CBA-316) feeder layer, following the manufacturer's protocol with minor modifications. The APS0004

cell line was provided by the RIKEN BRC through the National Bio-Resource Project of the MEXT, Japan. Cultures were fed daily and passaged at a split ratio of 1:8 when several colonies reached  $\approx 700 \mu\text{m}$  in diameter. The complete medium used constitutes Dulbecco's modified Eagle medium (Nacalai Tesque, Kyoto: 08459-35) with 15% (v/v) fetal bovine serum (JR Scientific, Woodland: 43640-500ESQ), 1% (v/v) non-essential amino acids (Nacalai Tesque, Kyoto: 06344-56), 0.1 mM 2-mercaptoethanol (Bio Basic, Markham: MB0338), and 0.1% (v/v) recombinant mouse inhibitory factors (Nacalai Tesque, Kyoto: NU0012-1). When required, cells were detached via accutase (Nacalai Tesque, Kyoto: 12679-54). Once stable culture was achieved, a line of the cultured cells was transferred into a feeder-free environment—onto gelatin-coated flasks and maintained with complete medium supplemented with 10  $\mu\text{M}$  ROCK Inhibitor Y-27632 (Stem Cell Technologies, Vancouver: 72302); the cells used for transplantation were cultured feeder-free for 8 passages to eliminate feeder residue cells.

## Mice

After the protocol was approved by the institute's research ethics committee, twenty-one clinically healthy 6-week old female BALB/c mice (Takrif Bistari Enterprise, Seri Kembangan) were acclimated to the laboratory for at least 7 days. The mice were caged individually in Super Rat 1400 cages, (Lab Products, Seaford) in an air-conditioned room. They were fed with autoclaved pellets (Specialty Feeds, Glen Forest) and sterile drinking water ad libitum; their bedding of wood shavings was replaced every 3 days. After acclimation, the mice were immunosuppressed by intramuscular injections of dexamethasone solution, 200  $\mu\text{g}/\text{mL}$  (a combination of 1 part Colvasone (Norbrook, Newry) and 9 parts 0.9% (w/v) sodium chloride solution (QR&C, Bangkok: S5068-1)); 5  $\mu\text{L}$  per g mouse weight (dosage: 1  $\mu\text{g}/\text{g}$  or 1 mg/kg), once a day for 3 consecutive days to prepare them for cell transplantation and avoid immune rejection [9]. On the final day, the mice were anaesthetized with 10 mg/mL Ketamil (Ilium, Glendenning) and 0.5 mg/mL Xylazil (Ilium, Glendenning) in sterile distilled water, 0.01 mL/g mice weight; and their lower backs were depilated with Nair hair removal cream.

## Wound Incision and APS0004 cell Transplantation

Wang et al.'s splinted wound mouse model was used for the protocol [10]. The mice were divided into 2 groups: Group A and Group B, with 9 mice each. For the baseline data of both groups, 3 clinically healthy female mice at the same age were processed for blood leucocyte count. A day after depilation, each mouse was anaesthetized and their lower back sterilized with povidone iodine and a wound was incised on each side of the vertebrae column, at the lower back; with a 5-mm biopsy punch (Premier, Plymouth Meeting: 9033516) and at a distance of at least 10 mm between the two wounds. For each mouse of Groups A and B, a total of 6 intradermal injections were made around the two wounds in a 3 (horizontal)  $\times$  2 (vertical) formation, with 20 mm between adjacent injections. Each injection for mice in Group A was 0.5 mL of freshly prepared APS0004 cell suspension ( $7 \times 10^5$  cells in 0.9% sodium chloride solution), while each injection for mice in Group B was 0.5 mL of 0.9% sodium chloride solution. Ring doughnut-shaped splints made of polyvinyl chloride sheets (with a diameter of 13-mm and an inner circle of 6-mm in diameter; sterilized with 0.5% sodium hypochlorite (Clorox, Oakland) and then with 70% ethanol) were adhered around the wounds with superglue. The wounds were then dressed with Tegaderm Transparent Film Dressing 1624W (3M, Saint Paul), and then with self-adhering bandage. The mouse was returned to its cage and allowed to regain consciousness.

## Euthanasia, Wound Bed Harvesting and Blood Harvesting

3 mice of each group (Groups A and B) were euthanized on day 7, 14, and 21. Approximately 0.5 mL blood was drawn from each mouse via cardiac puncture, then deposited and mixed into a 1.5-mL microcentrifuge tube with 40  $\mu\text{L}$  of 37.5 mg/mL EDTA solution. The right wound was excised together with surrounding tissue and spread on a piece of paper; the result is a rectangular-shaped skin tissue with the wound in the middle. The tissue sample was then stapled onto the cover of a histology cassette and snapped onto the cassette body. The

tissue sample was then fixed in 10% neutral buffered formalin (10% (v/v) formalin (Avantor, Radnor: 5016-08), 33.34 mM sodium phosphate (Merck, Kenilworth: 567549), and 45.79 mM di-sodium hydrogen phosphate (Merck, Kenilworth: 106585), in distilled water). The left wound bed was excised as well for the purpose of molecular biology studies which was scrapped due to resource constrains.

## Morphometry

The progression of wound closure of mice to be euthanized on day 14 was tracked with scaled photography on days 0, 3, 7, 10, and 14. For day 0, wound photos were taken right before application of Tegaderm; for day 3, 7, and 10, the mice were anesthetized before photography; for day 14, photos were taken after euthanasia. For photography, an EOS 550D camera (Canon, Tokyo) attached on a tripod facing downwards at approximately  $90^\circ$  was placed approximately 30 cm above the mouse. A photo was taken for each wound. For mice with splints fallen off, a replacement splint was placed upon the wound site before a photo was taken. For wound area estimation, the software GNU Image Manipulation Program (GIMP) 2.8.2.2 was used. Photos were opened with GIMP; using the Free Select Tool and Fuzzy Select Tool, the area within the splint's inner circle or the wound area was selected; the number of pixels selected displayed in the Histogram window was subsequently recorded. Using the area of the splint's inner circle as a scale, the wound area was approximated via the formulae:

$$\text{Wound Area} = \text{Wound Pixels} * \text{Splint Area} / \text{Splint Pixels}$$

Recovery percentage was calculated in respect to wound area on day 0. The data points were fitted with a sigmoid curve via the Boltzmann (Sigmoidal) function of the software SciDAVis 1.25.

## Blood Analyses

Blood total leukocyte count and differential leukocyte count were performed as part of the immune response evaluation. Both procedures were performed by independent laboratory, B.P. Clinical Lab, Malaysia. Total leukocyte count was performed via automated haematology analyser, KX-21 (Sysmex, Kobe). Differential blood count was performed by analysis of peripheral blood film.

## Histology Section Preparation

Each fixed wound bed sample was cut into 4 pieces with 3 incisions perpendicular to the anterior-posterior axis; the middle cut went through the wound centre, the other two cuts were in a way that the two middle pieces had the width about the height of a histology mould. The two middle pieces were placed into a cassette and moved into an automated tissue processor (Leica Biosystems, Wetzlar) for tissue processing with the following program: 2  $\times$  10% neutral buffered formalin for 1 h, 2  $\times$  95% ethanol (HmbG Chemicals, Germany) for 1 h, 3  $\times$  100% ethanol (J Kollin Chemicals, Midlothian) for 1 h, 2  $\times$  xylene (System, Shah Alam: XY433-90) for 1 h, 3  $\times$  paraffin wax (Leica Biosystems, Wetzlar: 39601006) for 1 h. The tissue samples were then embedded in paraffin wax. Sections were stained with H&E and Masson's Trichrome. Additional sections were immunohistochemically stained with monoclonal rabbit recombinant anti-CD31 (Abcam, Cambridge: ab182981) with the EXPOSE Mouse and Rabbit Specific HRP/DAB Detection Kit (Abcam, Cambridge: ab80436); and with monoclonal mouse anti-human CD68 (Agilent, Santa Clara: M0876) with the Animal Research Kit, Peroxidase (Agilent, Santa Clara: K3954).

## Wound Assessment via Histological Scoring

Stained sections were examined under a compound microscope (Olympus BX 40, Japan) at 100 $\times$  and 400 $\times$  (high power field (HPF)), and evaluated and scored (0 – 3 points) based on a scheme modified from that developed by Abramov et al. [11] and Loh et al. [12]. The scheme is described in detail in Table 1. The modifications were made to address several issues with the original schemes: (1) Assessment of reepithelialization, collagen, granulation tissue, and fibroblast are comparative in nature; a baseline score for unwounded skin was therefore added to better define the scheme. (2) With access to CD31-immunostaining, immature blood vessels that were otherwise hidden in

H&E staining came to light; to count every immature vessels would result in full scores in nearly all sections, in fact Altavilla et al. [13] in a histological assessment, only took into account mature vessels containing erythrocytes; however, to not count these immature vessels would not correctly reflect the state of angiogenesis; in a compromise, the scheme was adjusted to incorporate immature vessels into the mature vessel scheme. (3) Despite being an integral component of skin and playing a role in wound healing, the hypodermis was not taken in account in previous scoring schemes; as such, a variable that assessed adipocyte, hair buds, and sebaceous glands was added to the scoring scheme.

### Significance Testing

Wound closure as a whole was tested statistical significance between groups with a mixed-design analysis of variance (mixed-design ANOVA) using IBM SPSS Statistics 16.0.1. Additionally, wound area of each day, along with each type of blood leucocyte of each day, and each histological score of each day, were tested for statistical significance between groups with 2-tailed Welch's T-tests with Microsoft Excel version 16.0.13029.20232.  $p < 0.10$  was considered statistical significant for all comparisons; a larger p-value is used due to the small sample size [14].

**Table 1** Scheme for wound assessment via histological scoring.

Variable	Score			
	0	1	2	3
Epithelialization	None	Partial	Complete but immature or thin	Complete and mature
Collagen	None	Scant	Moderate (similar amount to unwounded skin)	Abundant
Blood vessels	None	≤5 vessels per HPF, or > 10 immature vessels per HPF, or both	6-10 vessels per HPF	>10 vessels per HPF
Granulation tissue	None (similar to unwounded skin)	Scant	Moderate	Abundant
Fibroblast	None to minimal	Few fibroblasts	More fibroblasts (similar amount to unwounded skin)	Predominantly fibroblasts
Neutrophils	None	0-25 neutrophils per HPF, scab neutrophil not counted	26-50 neutrophils per HPF, scab neutrophil not counted	>51 neutrophils per HPF, scab neutrophil not counted
Lymphocytes	None	0-25 lymphocytes per HPF	26-50 lymphocytes per HPF	>51 lymphocytes per HPF
Macrophages	None	0-25 macrophages per HPF	26-50 macrophages per HPF	>51 macrophages per HPF
Hypodermis	None	Few hair buds, or sebaceous glands, or indications of new adipocytes	Plenty of hair buds and sebaceous glands, plenty adipocytes yet not enough to 'bridge' adipocytes of both ends	Hair buds and sebaceous glands plentiful, adipocytes enough to bridge the wound; near indistinguishable from unwounded skin

\* Modified from the scheme developed by Abramov et al. [11] and Loh et al. [12]

## RESULTS AND DISCUSSION

The scores of the semi-quantitative assessment were quite varied in pattern (Fig. 1). Reepithelialization and hypodermis started low on day 7 and reached a full 3 marks, for at least one group, on day 21. Inflammatory variables such as neutrophil count and macrophage count started higher and dropped to 0 by day 14. Blood vessel amount, granulation tissue, and lymphocyte count began higher on day 7, but never reached 0. In contrast, Collagen started relatively low on day 7, but never reaches full score.

### Inflammation

Wound healing is classically divided into 3 or 4 phases [15–17]: homeostasis, inflammation, proliferation, and remodelling, in this order, with overlap between phases. The presence of neutrophils, macrophages, and lymphocytes in wound bed samples were assessed to investigate inflammation—the response to tissue damage caused by harmful stimuli—eliminating damaging agents, and repair and restore damaged tissue functionality [18].

Though they are interrelated, inflammation can be divided into acute and chronic in nature [18]; neutrophils are activated and migrated to the injured site in acute inflammation. At the injured site, neutrophils phagocytose necrotic tissue debris and pathogenic organisms. From

section evaluation, Group A sections scored a  $2.33 \pm 0.33$  while Group B sections scored a  $1.00 \pm 0$  on day 7 (Fig. 1). Sections of both groups scored a  $0 \pm 0$  on day 14 and day 21.

The scores of day 14 and day 21 suggest acute inflammation ended by day 14 for both groups. The presence of neutrophils in day 7 sections on the other hand suggests both groups are experiencing some stage of acute inflammation. Group A's significantly higher score ( $p = 0.0572$ ) suggests that they are closer to the peak of acute inflammation, while the lower score of the Group B would suggest it is reaching the end of acute inflammation.

It should be noted that neutrophils were also found in scabs as they were present in blood when the clot formed. These neutrophils were not counted in the section assessment as it is meant to reflect the day the wound sample was taken.

In contrast to acute inflammation, lymphocytes, macrophages and plasma cells predominate chronic inflammation [19], though this study focuses only on macrophages and lymphocytes as indicators of chronic inflammation.

Macrophages arrive at the injured site after neutrophils. Once activated, macrophages become effective at phagocytosing foreign organisms and secrete factors to control other inflammatory cells [19]. Scores of both groups are the same for all three periods:  $0.67 \pm 0.33$  for day 7 and  $0.00 \pm 0$  for day 14 and day 21 (Fig. 1).

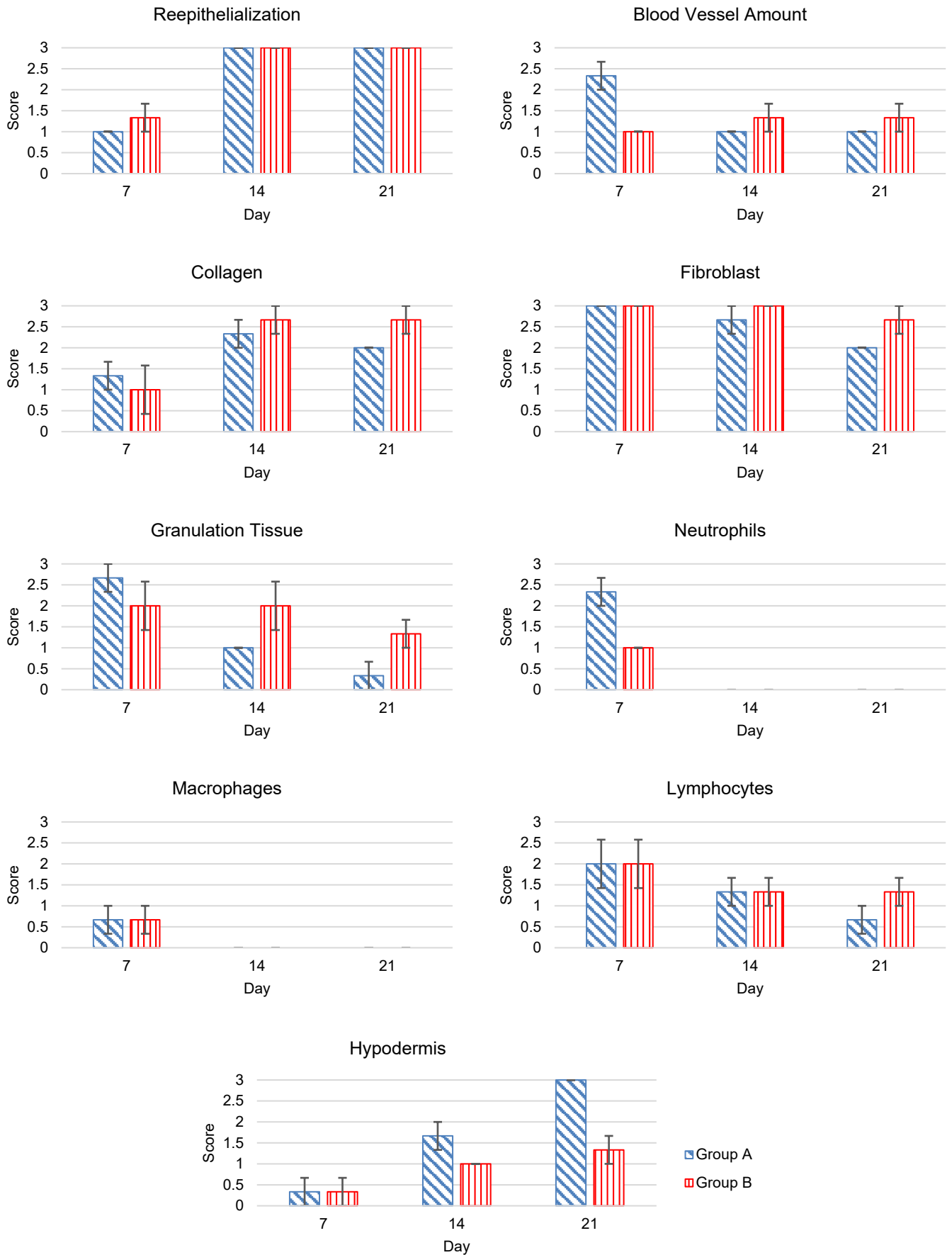


**Fig. 1** Wound assessment via histological scoring for days 7, 14, and 21 for the variables reepithelialization, collagen, blood vessel amount, granulation tissue, fibroblast, neutrophils, lymphocytes, macrophages, and hypodermis. Difference between groups was statistically significant for blood vessels day 7, neutrophils day 7, and hypodermis day 21; no significant differences were found in any other comparison

**Table 2** Leukocyte numbers of mice at various periods of the study. No significant differences were found between groups of each variable of each day.

Cell type	Typical values (2.5-97.5%)**		Baseline		Group A		Group B		
	Range	Mean	Day 0	Day 7	Day 14	Day 21	Day 7	Day 14	Day 21
Total Leukocyte	0.25-5.18	2.47	1.533 ± 0.352	3.867 ± 0.694	4.833 ± 1.794	4.733 ± 0.578	3.033 ± 0.821	3.833 ± 1.335	5.733 ± 0.731
Neutrophils	Percentage		24.9%	31.8%	37.4%	33.2%	41.6%	20.2%	34.1%
	Absolute number	0.02-1.12	0.41	0.382 ± 0.062	1.230 ± 0.238	1.807 ± 0.587	1.573 ± 0.319	1.261 ± 0.436	0.773 ± 0.037
Lymphocytes	Percentage		72.4%	66.0%	60.3%	65.4%	53.8%	74.0%	61.5%
	Absolute number	0.23-4.51	1.97	1.110 ± 0.294	2.553 ± 0.591	2.915 ± 1.450	3.096 ± 0.292	1.630 ± 0.408	2.838 ± 1.150
Monocytes	Percentage		2.2%	1.0%	2.3%	1.4%	4.7%	3.9%	4.1%
	Absolute number	0-0.09	0.02	0.033 ± 0.009	0.038 ± 0.007	0.111 ± 0.069	0.064 ± 0.020	0.141 ± 0.059	0.150 ± 0.088
Eosinophils	Percentage		0.5%	0.9%	0%	0%	0%	1.9%	0.3%
	Absolute number	0-0.21	0.05	0.007 ± 0.007	0.036 ± 0.036	0	0	0	0.073 ± 0.061
Basophils	Percentage		0%	0%	0%	0%	0%	0%	0%
	Absolute number	0-0.01	0	0	0	0	0	0	0

\*All absolute number values are expressed as mean ± standard error × 10<sup>3</sup> cells/μL; N = 3.

\*\*Values are for diet-restricted 7-10-week-old female CD-1 mice collected under isoflurane anesthesia; taken from the work of Bolliger et al. [22]

Lymphocytes are generally divided into T lymphocytes, B lymphocytes, and natural killer cells. While natural killer cells play a role in the innate immune system, T lymphocytes and B lymphocytes act as modulators in wound healing [20-21]. Section lymphocyte scores were highest on day 7 with 2.00 ± 0.67 for both groups (Fig. 1); for day 14 and day 21 sections, Group A sections scored 1.33 ± 0.33 and 0.67 ± 0.33 respectively, while Group B sections scored 1.33 ± 0.33 for both day 14 and day 21. Blood lymphocyte numbers on the other hand remain within typical numbers for both groups throughout the study (Table 2).

Judging from score alone, macrophage activation is believed to be immunosuppressed. Interestingly, this is in contrast to blood monocyte (macrophage precursor) numbers, with day 14 of Group B and day 7, day 14, and day 21 of Group A going above typical levels.

The higher lymphocyte score on day 7 would suggest some indication of chronic inflammation. Group A's score eventual descent to 0.67 ± 0.33 would suggest the exit of chronic inflammation, while Group B remaining on 1.33 ± 0.33 may suggest some complication in this respect, though the difference was not significant (p = 0.230). It should be noted however, that even without skin damage, lymphocytes would have a continued presence in skin as defence against pathogenic invasion, inflammatory conditions, and malignancy development [23]. In fact, while the number cannot be directly translated into mice, normal human skin has an estimated ~ 1 × 10<sup>6</sup> T cells/cm<sup>2</sup> [24].

Regarding the total and differential blood leucocyte count, no significant difference could be found between groups. However, there

was a dip in total leukocyte count on Day 0, yet the total leukocytes recovered in both groups since. Dexamethasone, the immunosuppressant administered in this study is likely the culprit; a large dose of hydrocortisone (a glucocorticoid similar to dexamethasone) causes leukopenia, intensifies until 24 hours, and persists until day 3 [25], consistent with our findings.

### Angiogenesis

Angiogenesis plays a pivotal role during the proliferation phase by providing capillaries, the means to transport oxygen and micronutrients to the recovering tissue and remove catabolic waste [26]. In fact, impaired angiogenesis can result in wounds turning chronic [27].

For the assessment of angiogenesis via the presence of blood vessels, Group A scored a 2.33 ± 0.33 on day 7 while Group B scored a 1.00 ± 0 (Fig. 1). The scores of both groups remained constant between day 14 and day 21, with Group B sections scoring 1.33 ± 0.33 and Group A sections scoring 1.00 ± 0.

While the differences in score between groups on day 14 and 21 are quite small and not significant (p = 0.423 for both), the difference in score on day 7 was significant (p = 0.057). The higher score would suggest angiogenesis may be closer to the peak in Group A sections as compared to Group B sections. Considering that wounds have yet to closed on day 7 (Fig. 4 and Fig. 5), it can only be assumed that angiogenesis had barely started in Group B sections, as opposed to the scenario where angiogenesis had passed its peak and blood vessels have already been removed in the remodelling phase.

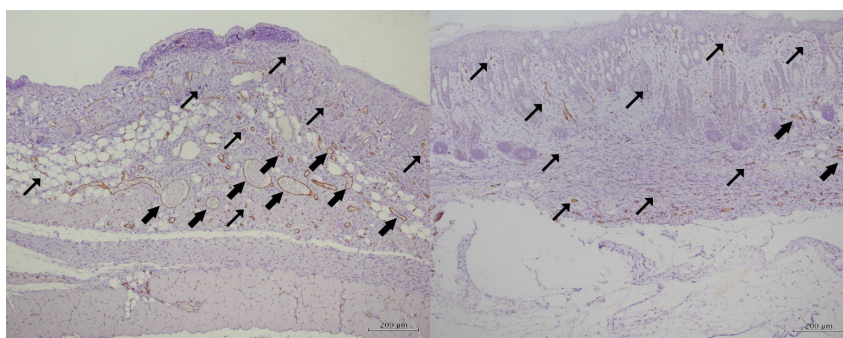


**Fig. 2** Micrograph representation of CD-31 immunostained sections, at 100 × magnification. Endothelial cells that line blood vessels are stained brown. (Left) Group A section at day 7, (right) Group B section at day 7. Thin arrows indicate immature or small vessels, thick arrows indicate mature or large vessels; though there are too many vessels to point out all.

This trend of decline in blood vessel score after the initial bloom of angiogenesis on day 7 is expected; new blood vessels form to transport oxygen and micronutrients early in wound healing; when wound healing enters the remodelling phase, excessive blood vessels are no longer needed and therefore removed [28].

In a similar stem cell-based study, a bone marrow-impregnated collagen matrix significantly increased blood vessel density on days 3, 5, and 7 mouse wounds but not day 10 [3]; in another, the use of CD34+ peripheral blood mononuclear cells on diabetic mice resulted in greater vascularization on days 7 and 14, but not day 21 [29]. These findings are similar with ours.

Interestingly, another research group noted an increase in blood vessel size when they applied non-diabetic mouse hematopoietic progenitor cells to wounds [30], though the difference was not significantly proven. The same could be observed on sections of Group A on day 7 in this study (Fig. 2).

### Fibroblast Proliferation

In wound healing, fibroblasts play the role of breaking down fibrin clots, contracting wounds, and depositing extracellular matrix and collagen to support wound healing-associated cells [31].

In the assessment, both groups scored  $3.00 \pm 0$  for day 7 (Fig. 1). For day 14, Group B sections maintain a  $3.00 \pm 0$  while Group A section scored a  $2.67 \pm 0.33$ . For day 21, Group A's score lowered again to  $2.00 \pm 0$  while Group B fibroblast score reduced to  $2.67 \pm 0.33$ .

Loh et al.'s scheme [12], in which this variable's scoring is based on, examined fibroblast amount as an indication of scarring [12]. However, according to Jiang et al., while fibroblasts (together with keratinocytes) do play a central role in scar formation, it is the balance of signalling pathways that determine the outcome of wound healing [32]. That being said, fibroblast amount can be an indication of the phase of wound healing.

Both groups started at a score of 3 on day 7, an indication of fibroblast proliferation relatively early in wound healing. The scores of both groups reduced over time, though by day 21, only Group A's score has reached 2, the baseline score for unwounded skin, whereas Group B has not. The difference was not significant ( $p = 0.184$ ) however.

### Granulation Tissue

Granulation tissue is essentially an infill of macrophages, fibroblasts, and blood vessels, in the wound area to deposit an extracellular matrix to support of the growth of more granulation and to stimulate wound contraction [33].

In this assessment, for days 7, 14, and 21, Group A sections scored  $2.67 \pm 0.33$ ,  $1.00 \pm 0$ , and  $0.33 \pm 0.33$  respectively, while Group B sections scored  $2.00 \pm 0.67$  for both day 7 and day 14, and  $1.33 \pm 0.33$  for day 21 (Fig. 1).

Like the scoring of blood vessels and fibroblast amount, a higher score is desirable in the earlier stages of wound healing as it is indicative of the proliferation phase. Unlike blood vessels and fibroblast however, granulation tissue does not exist in unwounded skin; therefore, in the later stages, a lower score is preferable as it indicates that granulation tissue has been replaced by collagen, a process that occurs in the remodelling phase.

With this in mind, the scores is in favour Group A sections with the score for day 7 being higher, yet lower on day 14 and day 21 sections, with the later nearing 0; though the differences were not considered significant ( $p = 0.387$  for day 7,  $p = 0.225$  for day 14,  $p = 0.101$  for day 21).

### Collagen Deposition

As discussed earlier, fibroblasts deposit collagen into the wound and replace granulation tissue. The deposition and remodelling of collagen plays a role in providing tensile strength to the wound [34].

In the assessment, for days 7, 14, and 21, Group A sections scored  $2.33 \pm 0.33$ ,  $2.33 \pm 0.33$ , and  $2.00 \pm 0$  respectively; Group B sections on the other hand scored  $1.00 \pm 0.67$  for day 7, and  $2.67 \pm 0.33$  for both day 14 and day 21 (Fig. 1).

While fibroblast amount and granulation tissue scores are highest for day 7, collagen, the product, is lowest on day 7; collagen peaked on day 14 where the score is highest. Group A sections scored slightly higher for day 7, suggesting they are ahead in the proliferation phase. For day 14, Group A sections scored lower than Group B sections, but this is because the remodelling has begun to some degree; the high hypodermis regeneration score suggest that the deposited collagen is being removed, and in its place the return of adipocytes, hair follicles, and sebaceous glands.

For day 21, Group A sections scored a  $2.00 \pm 0$ , which is the baseline score for unwounded skin, and an indication that remodelling is near its end. Group B sections however maintained a  $2.67 \pm 0.33$ , meaning there is still plenty of excess collagen fibre. The difference between groups was not significant however, with  $p = 0.649$  for day 7,  $p = 0.519$  for day 14, and  $p = 0.18$  for day 21.

Interestingly, panniculus carnosus, the striated muscle under the hypodermis appears to be 'blotted' in both groups on day 14 (Fig. 3), comprised mainly of collagen with small bundles of muscles intermingled, especially in the centre.

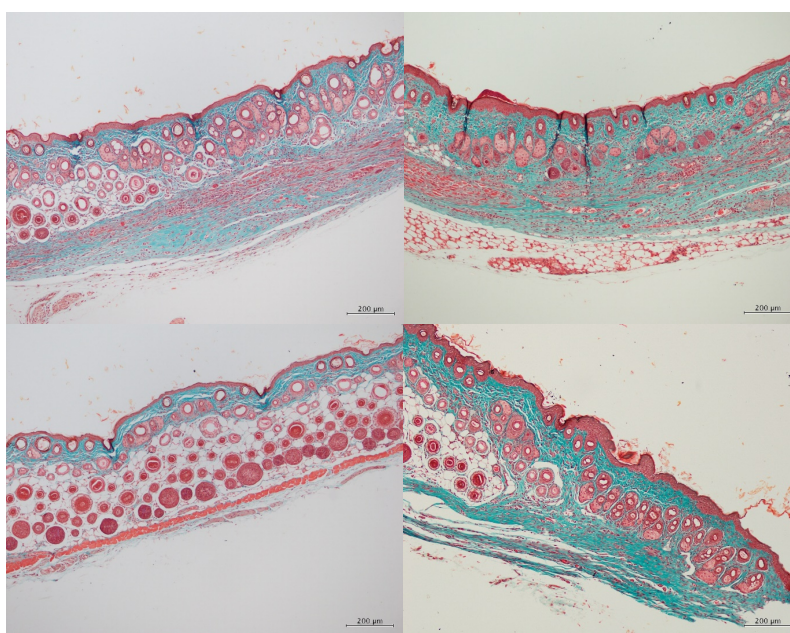


**Fig. 3** Micrograph representation of Masson's Trichrome-stained sections, at 100 × magnification. Collagen is stained blue. (Top left) Group A day 14, (top right) Group B day 14, (bottom left) Group A day 21, (bottom right) Group B day 21.

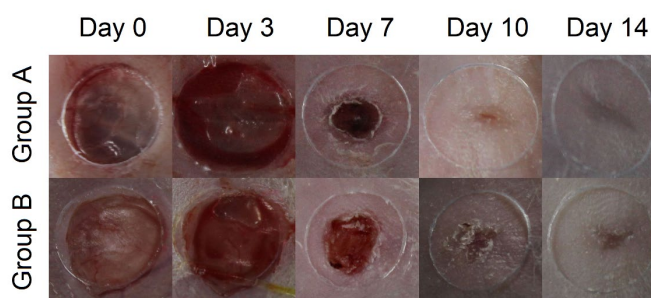


Fig. 4 Photographical representation of wound healing in mice.

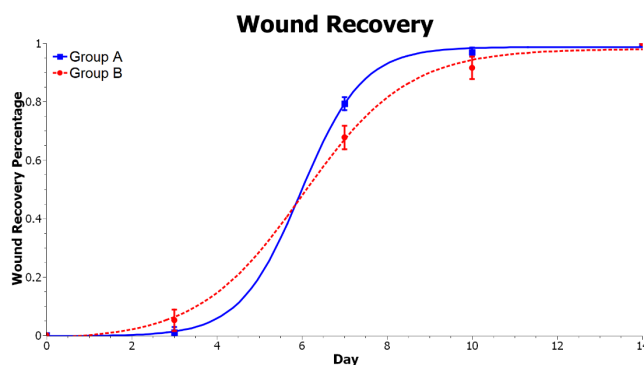


Fig. 5 Comparison of wound closure between Groups A and B over time.

Table 3 Multivariate Tests Component of the Mixed-design ANOVA

Effect		Value	F	Hypothesis df	Error df	Sig.	Partial Eta Squared
Day	Pillai's Trace	.999	3.809E3	3.000	8.000	.000	.999
	Wilks' Lambda	.001	3.809E3	3.000	8.000	.000	.999
	Hotelling's Trace	1428.403	3.809E3	3.000	8.000	.000	.999
	Roy's Largest Root	1428.403	3.809E3	3.000	8.000	.000	.999
Day * Group	Pillai's Trace	.464	2.307 <sup>a</sup>	3.000	8.000	.153	.464
	Wilks' Lambda	.536	2.307 <sup>a</sup>	3.000	8.000	.153	.464
	Hotelling's Trace	.865	2.307 <sup>a</sup>	3.000	8.000	.153	.464
	Roy's Largest Root	.865	2.307 <sup>a</sup>	3.000	8.000	.153	.464

a. Exact statistic

### Reepithelialization and Wound Closure

Comparing wound closure via graph plotted with Boltzmann function in SciDAVis, as illustrated in Fig. 5, it would appear the Group A's curve is slightly stiffer than that of Group B. However, the mixed-design ANOVA (Table 3) indicated the difference between groups as a whole was not significant ( $p = 0.153$ ). While unfortunate, this is consistent with the results of a study that transplanted ES cells in diabetic rats [7]. The Mauchly's test of sphericity (a component of mixed-design ANOVA) resulted in a  $p = 0$ , indicating that sphericity has been violated and the mixed-design ANOVA is prone to type 1 error (false positive). When compared on independent days, wound closure was significantly different on day 7 ( $p = 0.038$ ).

Reepithelialization is slightly different from wound closure as shown in Fig. 1. While both groups score a full  $3.00 \pm 0$  in day 14 and day 21, for day 7, Group B's wounds have a mean score of  $1.33 \pm 0.33$  while Group A wounds only scored  $1.00 \pm 0$ ; the difference was not significant however ( $p = 0.374$ ).

### Hypodermis Regeneration

Hypodermis, the deepest layer of skin is home to adipose tissue and skin appendages such as hair follicles, sebaceous gland, and sweat glands [35]; though sweat glands are absent from mouse skin for the most part [36]. Adipocytes of the adipose tissue play a role in fibroblast recruitment during wound healing [37]. In the proliferation phase, adipocyte precursor cells are activated to differentiate into adipocytes to repopulate the hypodermis [37].

For hypodermis assessment, sections only scored  $0.33 \pm 0.33$  for both groups on day 7. On day 14, Group A sections scored  $1.67 \pm 0.33$  while Group B sections scored only  $1.00 \pm 0$ , the difference was not significant however ( $p = 0.184$ ). The difference was significant on day 21 ( $p = 0.006$ ) where Group A sections scored a full  $3.00 \pm 0$  while Group B sections scored only  $1.33 \pm 0.33$ .

Much of the collagen, most notably in day 14 sections, was deposited in the area that would otherwise be the hypodermis of unwounded skin. As discussed earlier, hypodermis regeneration is to some extent, concurrent with the remodelling phase when excess collagen and blood vessels are removed.

For hypodermis, 3 marks is the baseline for unwounded skin, therefore the fact that Group A sections scored 3 on day 21 suggests Group A's wound healing is complete or at least near complete,

whereas the  $1.33 \pm 0.33$  score of Group B sections suggests their sections may still be in the middle of the remodelling phase.

### CONCLUSION

The semiquantitative assessment of wound sections based on a scoring scheme suggests that Group A wounds (APS0004 cell-transplanted group) fared significantly better in angiogenesis and hypodermis regeneration, indicative that Group A wounds were ahead in the progression of wound healing. Additionally, lymphocyte count, fibroblast count, granulation tissue, collagen, and wound closure, seem to support this notion, although the differences between group was not enough to be considered significant. Group B (the control group) scored significantly higher in neutrophil count on day 7, indicative of exiting acute inflammation and ahead in this respect.

### ACKNOWLEDGEMENT

We would like to thank Dr Suvik Assaw, Mr Khairil Azlan Bahrin, and Mr Muhamad Fakhri for technical assistance. For other types of assistance, we would like to thank Dr Maheza, Assoc Prof Mun Kein Seong, and Ms Teh Liam Chee.

For funding, a portion of the study was self-funded, while the rest was funded by donations; donors include Selvaraj Y Subramaniam, Sri Ternak Food Mart Sdn Bhd, Dato Simon Chong, Choong Siew Khay, Irene Ong, Hen Kee Restaurant, Andy and Su Ying, Sam and Yaw Chong, Kate, Sui Kok Hong, Terrence Ong, Yuan Hui Fang, Farah Izana, Chua Hui Mei, Sze Pow Lean, Sze Soo Lein, Lai Chin Mei, Fei Lo, Sze Chong Boon, Wilson Cheng, Sze Chong Wei, and 4 others who choose to remain anonymous. We would also like to thank the Society for Anti-Aging, Aesthetic and Regenerative Medicine Malaysia for their endorsement.

### REFERENCES

- [1] Badiavas, E. V.; Falanga, V. Treatment of chronic wounds with bone marrow-derived cells. *Archives of Dermatology* 2003, 139, 510–516.
- [2] Borue, X.; Lee, S.; Grove, J.; Herzog, E. L.; Harris, R.; Diflo, T.; Glusac, E.; Hyman, K.; Theise, N. D.; Krause, D. S. Bone marrow-derived cells contribute to epithelial engraftment during wound healing. *The American Journal of Pathology* 2004, 165, 1767–1772.

- [3] Ichioka, S.; Kouraba, S.; Sekiya, N.; Ohura, N.; Nakatsuka, T. Bone Marrow-impregnated collagen matrix for wound healing: experimental evaluation in a microcirculatory model of angiogenesis, and clinical experience. *British Journal of Plastic Surgery* 2005, 58, 1124–1130.
- [4] Sasaki, M.; Abe, R.; Fujita, Y.; Ando, S.; Inokuma, D.; Shimizu, H. Mesenchymal stem cells are recruited into wounded skin and contribute to wound repair by transdifferentiation into multiple skin cell type. *The Journal of Immunology* 2008, 180, 2581–2587.
- [5] Yoshikawa, T.; Mitsuno, H.; Nonaka, I.; Sen, Y.; Kawanishi, K.; Inada, Y.; Takakura, Y.; Okuchi, K.; Nonomura, A. Wound therapy by marrow mesenchymal cell transplantation. *Plastic and Reconstructive Surgery* 2008, 121, 860–877.
- [6] Lambert, A. P. F.; Zandonai, A. F.; Bonatto, D.; Machado, D. C.; Henriques, J. A. P. Differentiation of human adipose-derived adult stem cells into neuronal tissue: Does it work? *Differentiation* 2009, 77, 221–228.
- [7] Lee, K.-B.; Choi, J.; Cho, S.-B.; Chung, J.-Y.; Moon, E.-S.; Kim, N.-S.; Han, H.-J. Topical embryonic stem cells enhance wound healing in diabetic rats. *Journal of Orthopaedic Research* 2011, 29, 1554–1562.
- [8] Takahashi, K.; Yamanaka, S. Induction of pluripotent stem cells from mouse embryonic and adult fibroblast cultures by defined factors. *Cell* 2006, 126, 663–676.
- [9] Zamri-Saad, M.; Effendy, A. The effects of dexamethasone on the response of bronchus-associated lymphoid tissue to intranasal administration of formalin-killed *Pasteurella haemolytica* A2 in goats. *Veterinary Research Communications* 1999, 23, 467–473.
- [10] Wang, X.; Ge, J.; Tredget, E. E.; Wu, Y. The mouse excisional wound splinting model, including applications for stem cell transplantation. *Nature Protocols* 2013, 8, 302–309.
- [11] Abramov, Y.; Webb, A. R.; Miller, J.-J. R.; Alshahrour, A.; Botros, S. M.; Goldberg, R. P.; Ameer, G. A.; Sand, P. K. Biomechanical characterization of vaginal versus abdominal surgical wound healing in the rabbit. *Am. Journal of Obstetrics and Gynaecology* 2006, 194, 1472–1477.
- [12] Loh, E. Y. X.; Fauzi, M. B.; Ng, M. H.; Ng, P. Y.; Ng, S. F.; Amin, M. C. I. M. Insight into delivery of dermal fibroblast by non-biodegradable bacterial nanocellulose composite hydrogel on wound healing. *International Journal of Biological Macromolecules* 2020.
- [13] Altavilla, D.; Saitta, A.; Cucinotta, D.; Galeano, M.; Deodato, B.; Colonna, M.; Torre, V.; Russo, G.; Sardella, A.; Urna, G.; et al. Inhibition of lipid peroxidation restores impaired vascular endothelial growth factor expression and stimulates wound healing and angiogenesis in the genetically diabetic mouse. *Diabetes* 2001, 50, 667–674.
- [14] Kim, J. H.; Choi, I. Choosing the level of significance: A decision-theoretic approach. *Abacus* 2019
- [15] Singer, A. J.; Clark, R. A. Cutaneous wound healing. *New England Journal of Medicine* 1999, 341, 738–746.
- [16] Sonnemann, K. J.; Bement, W. M. Wound Repair: Toward understanding and integration of single and multicellular wound responses. *Annual Review of Cell and Developmental Biology* 2011, 27, 10.1–10.27.
- [17] Shaw, T. J.; Martin, P. Wound repair at a glance. *Journal of Cell Science* 2009, 122, 3209–3213.
- [18] O'Dowd, G.; Bell, S.; Wright, S. *Acute inflammation, Healing and Repair*. In *Wheater's Pathology: A text, atlas and review of histopathology*; Elsevier: Edinburgh, 2020; pp. 22–36.e9.
- [19] O'Dowd, G.; Bell, S.; Wright, S. *Chronic inflammation*. In *Wheater's Pathology: A text, atlas and review of histopathology*; Elsevier: Edinburgh, 2020; pp. 37–46.e13.
- [20] Schaffer, M.; Barbul, A. Lymphocyte function in wound healing and following injury. *British Journal of Surgery* 1998, 85, 444–460.
- [21] Sirbulescu, R. F.; Boehm, C. K.; Soon, E.; Wilks, M. Q.; Ilieș, I.; Yuan, H.; Maxner, B.; Chronos, N.; Kaittanis, C.; Normandin, M. D.; et al. Mature B cells accelerate wound healing after acute and chronic diabetic skin lesions. *Wound Repair and Regeneration* 2017, 25, 774–791.
- [22] Bolliger, A. P.; Everds, N. E.; Zimmerman, K. L.; Morre, D. M.; Smith, S. A.; Barnhart, K. F. *Hematology of laboratory animals*. In *Schalm's Veterinary Hematology*; Weiss, Douglas J and Wardrop, K Jane, Ed.; Wiley-Blackwell: State Avenue, 2010; pp. 852–887.
- [23] Lafouresse, F.; Groom, J. R. A task force against local inflammation and cancer: Lymphocyte trafficking to and within the skin. *Frontiers in Immunology* 2018, 9, 2454.
- [24] Clark, R. A.; Chong, B.; Mirchandani, N.; Brinster, N. K.; Yamanaka, K.; Dowgiert, R. K.; Kupper, T. S. The vast majority of CLA+ T cells are resident in normal skin. *The Journal of Immunology* 2006, 176, 4431–4439.
- [25] Maianski, D. N.; Makarova, O. P. The effect of hydrocortisone on neutrophil functional activity. *Bulletin of Experimental Biology and Medicine* 1989, 108, 730–732.
- [26] Honnegowda, T. M.; Kumar, P.; Udupa, E.; Kumar, S.; Kumar, U.; Rao, P.; others. Role of angiogenesis and angiogenic factors in acute and chronic wound healing. *Plastic and Aesthetic Research* 2015, 2, 243–249.
- [27] Demidova-Rice, T. N.; Durham, J. T.; Herman, I. M. Wound healing angiogenesis: Innovations and challenges in acute and chronic wound healing. *Advances in Wound Care* 2012, 1, 17–22.
- [28] Suzuki, J. B.; Resnik, R. R. Wound Dehiscence: *Incision line opening*. In *Misch's Avoiding Complications in Oral Implantology*; Elsevier, 2018; pp. 402–439.
- [29] Sivan-Loukianova, E.; Awad, O. A.; Stepanovic, V.; Bickenbach, J.; Schattman, G. C. CD34+ blood cells accelerate vascularization and healing of diabetic mouse skin wounds. *Journal of Vascular Research* 2003, 40, 368–377.
- [30] Stepanovic, V.; Awad, O.; Jiao, C.; Dunnwald, M.; Schattman, G. C. Lep<sup>rd</sup> diabetic mouse bone marrow cells inhibit skin wound vascularization but promote wound healing. *Circulation Research* 2003, 92, 1247–1253.
- [31] Bainbridge, P. Wound healing and the role of fibroblasts. *Journal of Wound Care* 2013, 22.
- [32] Jiang, D.; Rinkevich, Y. Scars or Regeneration?—Dermal fibroblasts as drivers of diverse skin wound responses. *International Journal of Molecular Sciences* 2020, 21, 617.
- [33] Pratt, J.; West, G. *Pressure Therapy: History and rationale. in pressure garments: A manual on their design and fabrication*; Butterworth-Heinemann: Linacre House, 2014; pp. 1–21.
- [34] Rangaraj, A.; Harding, K.; Leaper, D. Role of collagen in wound management. *Wounds UK* 2011, 7, 54–63.
- [35] O'Dowd, G.; Bell, S.; Wright, S. *Infections of histological importance*. In *Wheater's Pathology: A Text, Atlas and Review of Histopathology*; Elsevier: Edinburgh, 2020; pp. 47–64.e14.
- [36] Lu, C.; Fuchs, E. sweat gland progenitors in development, homeostasis, and wound repair. *Cold Spring Harbor Perspectives in Medicine* 2014, 4, a015222.
- [37] Rivera-Gonzalez, G.; Shook, B.; Horsley, V. Adipocytes in skin health and disease. *Cold Spring Harbor Perspectives in Medicine* 2014, 4, a015271.